



**HAL**  
open science

## Ab initio tensile experiment on a model of an intergranular glassy film in $\beta$ -Si<sub>3</sub>N<sub>4</sub> with prismatic surfaces

W.Y. Ching, Paul Rulis, Lizhi Ouyang, Anil Misra

► **To cite this version:**

W.Y. Ching, Paul Rulis, Lizhi Ouyang, Anil Misra. Ab initio tensile experiment on a model of an intergranular glassy film in  $\beta$ -Si<sub>3</sub>N<sub>4</sub> with prismatic surfaces. Applied Physics Letters, 2009, pp.051907-1 - 051907-3. hal-00556118

**HAL Id: hal-00556118**

**<https://hal.science/hal-00556118>**

Submitted on 15 Jan 2011

**HAL** is a multi-disciplinary open access archive for the deposit and dissemination of scientific research documents, whether they are published or not. The documents may come from teaching and research institutions in France or abroad, or from public or private research centers.

L'archive ouverte pluridisciplinaire **HAL**, est destinée au dépôt et à la diffusion de documents scientifiques de niveau recherche, publiés ou non, émanant des établissements d'enseignement et de recherche français ou étrangers, des laboratoires publics ou privés.

# Ab initio tensile experiment on a model of an intergranular glassy film in $\beta$ -Si<sub>3</sub>N<sub>4</sub> with prismatic surfaces

W. Y. Ching,<sup>1,a)</sup> Paul Rulis,<sup>1</sup> Lizhi Ouyang,<sup>2</sup> and A. Misra<sup>3</sup>

<sup>1</sup>Department of Physics, University of Missouri-Kansas City, Kansas City, Missouri 64110, USA

<sup>2</sup>Department of Physics & Mathematics, Tennessee State University, Nashville, Tennessee 37221, USA

<sup>3</sup>Department of Civil, Environmental and Architectural Engineering, University of Kansas, Lawrence, Kansas 66045, USA

(Received 18 December 2008; accepted 19 January 2009; published online 5 February 2009)

We report the results of a large-scale *ab initio* simulation of an intergranular glassy film (IGF) model in  $\beta$ -Si<sub>3</sub>N<sub>4</sub>. It is shown that the stress-strain behavior under uniaxial load in the model with prismatic surfaces and few defective bonds is very different from an earlier IGF model with basal planes. The results are explained by the fundamental electronic structure of the model. © 2009 American Institute of Physics. [DOI: 10.1063/1.3079800]

It is now well recognized that the mechanical properties of polycrystalline ceramics are controlled by its microstructures such as the nanometer thick intergranular glassy films (IGFs). The presence and the physical properties of IGFs in a number of different ceramic materials have been a subject of many experimental and theoretical investigations.<sup>1</sup> However, such investigations are extremely challenging because of the complexity of the IGF structure. Experimentally, it is difficult to fully characterize the samples and carry out measurements aimed specifically at a particular aspect of the IGF. Theoretically, the ability to reveal the complicated structure-property relationship is hindered by the absence of well constructed IGF models and the accuracy limitations of various theories. In recent years, there has been considerable development in using *ab initio* methods based on density functional theory (DFT) to simulate the mechanical properties of ceramic crystals.<sup>2</sup> We have demonstrated that such an approach can be applied to IGF models in  $\beta$ -Si<sub>3</sub>N<sub>4</sub> which have yielded a wealth of previously unknown information.<sup>3-6</sup> The model we previously constructed has 798 atoms sandwiched between the basal planes of  $\beta$ -Si<sub>3</sub>N<sub>4</sub> with an IGF region consisting of Si, O, and N ions and a width of about 1 nm [Fig. 1(a), basal model]. Theoretical tensile experiments were carried out on both the pure [no rare earth (RE) additives] and Y-doped models.<sup>4</sup> It was concluded that the behavior of the mechanical deformation is highly nonlinear in clear violation of the Cauchy Born theory routinely accepted by the engineering community. It was also shown that Y-doping enhances the mechanical properties of the IGF in the form of increased maximum strain and stress as compared to the undoped model consistent with experimental observations.<sup>7</sup>

In this letter, we report the results of a theoretical tensile experiment on a new IGF model with prismatic planes instead of basal planes. This model (prismatic model) is more realistic since most IGFs observed in polycrystalline  $\beta$ -Si<sub>3</sub>N<sub>4</sub> have prismatic planes.<sup>8</sup> This 907-atom model with periodic boundary conditions [see Fig. 1(b)] was constructed in a similar manner as in the basal model and was fully relaxed using the Vienna *ab initio* simulation package (VASP).<sup>9</sup> The IGF region (defined as the region roughly between the crystalline Si layers) is about 1.7 nm wide and contains 12 N ions

in the interior of IGF. The equilibrium cell dimension is  $14.554 \times 15.225 \times 47.420 \text{ \AA}^3$  with the  $z$ -axis perpendicular to the IGF layer. This is a fairly ideal model with a few defective structures in contrast to the basal model. At the crystal/glass interface, the terminal Si (N) atoms from the crystal layer form rather normal bonds with O (Si) in the glassy region in almost equal proportions. Such a near-perfect interfacial structure has been observed in high resolution electron microscopy images in some RE-doped samples.<sup>10-12</sup> All Si-O and Si-N bond distances are very reasonable with a few bonds as large as  $1.87 \text{ \AA}$ . The IGF region in the prismatic model contains 72 Si, 124 O, and 32 N ions (including the terminal N from the crystal part). Among them, there are only three threefold and one fivefold Si atoms, eight twofold N atoms, and two threefold O atoms. Hence the glassy region in the present model has a fairly low defect density, assuming the ideal bonding to be fourfold for Si, threefold for N, and twofold for O.

The theoretical tensile experiment was carried out by systematic extension of the model in the  $z$  direction in small steps with the  $x$ - $y$  dimensions kept fixed. During each exten-

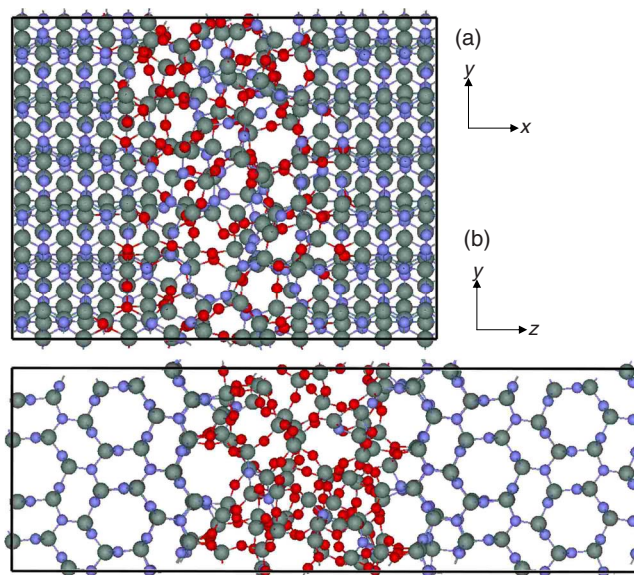


FIG. 1. (Color online) Comparison of the two IGF models in  $\beta$ -Si<sub>3</sub>N<sub>4</sub>: (a) the 798 atom basal model and (b) the 907-atom prismatic model.

<sup>a)</sup>Electronic mail: chingw@umkc.edu.

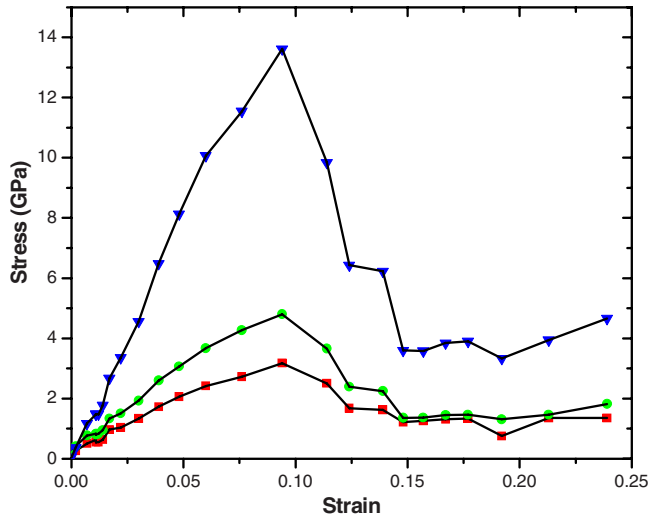


FIG. 2. (Color online) Stress vs strain of the prismatic model under uniaxial extension in the  $z$ -direction. Each data point is collected after full *ab initio* relaxation using VASP at a given strain. The  $xx$  and  $yy$  components of the strain are also shown.

sion step, the model is fully relaxed using VASP until the desired convergence was reached. We used the ultrasoft generalized gradient approximation potential with 1 k point and an energy cutoff of 400 eV. The electronic energy and force convergences were set at 0.001 and 0.01 eV/Å, respectively. The extension steps were repeated until the model was fully fractured and well separated. The total energy, the stress, and the atomic configuration at each step were registered at 22 data points. Figure 2 shows the stress versus strain data for the three Cartesian components  $\sigma_{zz}$ ,  $\sigma_{xx}$ , and  $\sigma_{yy}$  from the tensile experiment. Note that the strain ( $s$ ) is defined as the percentage of extension of the entire supercell in the  $z$  direction. The  $zz$  stress component is larger than the  $xx$  and  $yy$  components since the load is applied in the  $z$  direction and the  $x$ - $y$  dimension is kept fixed. This corresponds to the so-called “uniaxial extension” which induces a triaxial stress state.<sup>2</sup> The stress-strain response has interesting features in both pre- and postfailure regions. The prepeak response is nonlinear; however, the failure is considerably more abrupt than that reported for perfect crystals.<sup>13</sup> The maximum stress of 13.6 GPa for  $\sigma_{zz}$  occurs at the strain of 9.4%. In contrast, peak stress for perfect crystals has been reported to be as high as 75 GPa at strains  $>25\%$ . Beyond the peak at  $s=0.094$ ,  $\sigma_{zz}$  drops rapidly but not to zero as would be expected from fracture mechanics of brittle materials. Even at  $s=0.24$ , where the IGF model is fully fractured, there remains a sizable stress of roughly 1/3 of the maximum value. It is observed that the stress at  $s$  greater than 0.20 actually increases slightly when the film is already broken. This is most likely due to the extremely slow convergence in the relaxation process which would require far more steps when the vacuum region is created after the fracture of IGF. Additional work is necessary to confirm this point.

Figure 3 shows the atomistic pictures of the IGF model at five different strains of  $s=0.0, 0.39, 0.094, 0.148,$  and  $0.24$ , respectively. It is clear that, initially, the applied strain simply elongates the Si–O and Si–N bonds within the IGF. Near the maximum stress, some bonds start to break and the atoms with the breaking bonds recoil back in the opposite direction. At the largest strain simulated ( $s=0.24$ ), the two

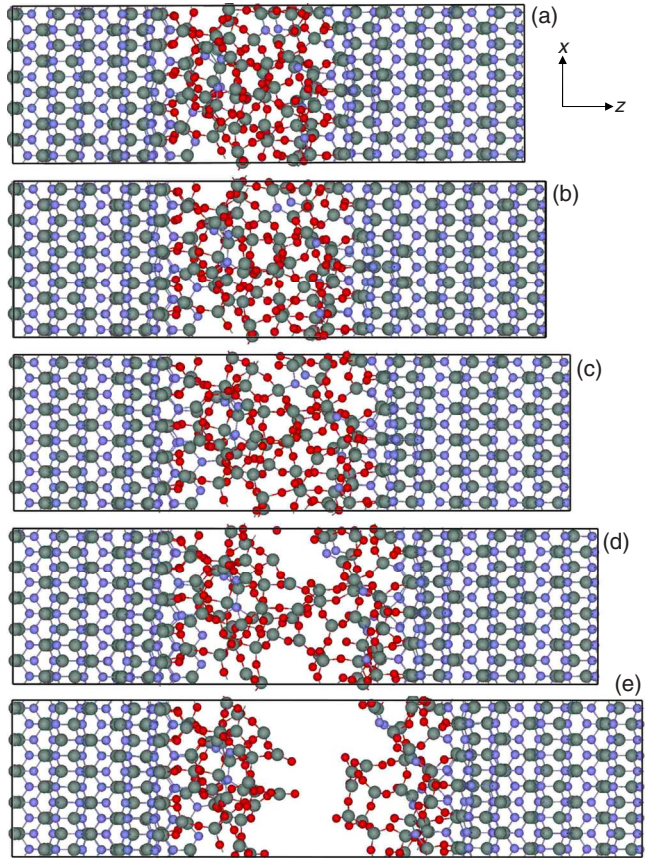


FIG. 3. (Color online) Atomic structures of the prismatic model under strains of (a) 0.00, (b) 0.039, (c) 0.094, (d) 0.148, and (e) 0.239.

parts of the model were clearly separated and the model resembles two  $\beta$ -Si<sub>3</sub>N<sub>4</sub> (01-10) surfaces coated with glassy films. The fracture occurs at the interior of the IGF, presumably at the location with lower bond density, not at the interface between the IGF and the crystal. This behavior is very different from the earlier study on the basal model where the fracture occurs at the IGF crystal interface and the stress drops to zero after fracture.<sup>4,6</sup>

The electronic structure of the prismatic IGF model under strain is studied by the first-principles orthogonalized linear combination of the atomic orbitals (OLCAO) method.<sup>14</sup> The DFT-based OLCAO method with atomic orbitals used in the basis expansion is highly accurate and efficient for large complex structures. In the present calculation, a full basis set is used<sup>15</sup> and the full secular equation of dimension  $9111 \times 9111$  is diagonalized to obtain all energy eigenvalues and wave functions. Figure 4 shows the calculated density of states (DOS) of the model at five different strains. At zero strain, a sizable gap of about 3.8 eV is evident. There exist a few defective states in the gap near the valence band (VB) and the conduction band (CB) edges. These defect states can be traced to the few under- or over-coordinated atoms discussed above. As the strain is increased, more defective states move toward the center of the gap, signaling an increase in defects due to bond distortion or bond breaking. After fracture, these defective states move back to the proximity of the VB and CB band edges as surface states. A surprising fact is that the overall DOS features vary little with strain except for the location of the defective states.

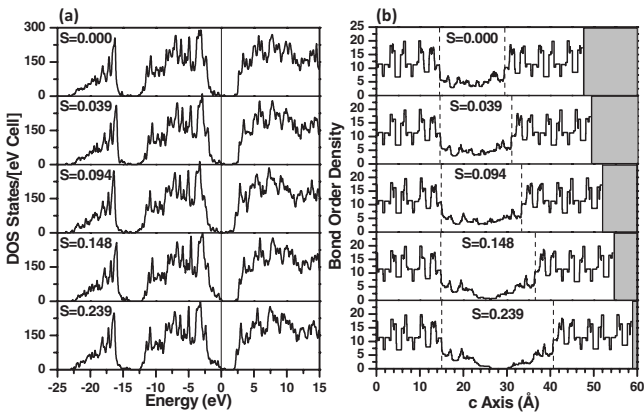


FIG. 4. (a) Calculated DOS and (b) BOD for the prismatic model under various uniaxial strains. The zero of the energy is set at the topmost occupied state.

One of the special advantages of the OLCAO method is that quantitative information on the bond strength can be obtained using the Mulliken scheme<sup>16</sup> and a separate minimal basis calculation. The bond order (BO) between a pair of atoms is defined as

$$\rho_{\alpha\beta} = \sum_{n, occ} \sum_{i, j} C_{i\alpha}^{*n} C_{j\beta}^n S_{i\alpha, j\beta}$$

where  $i$  and  $j$  labels are the orbital quantum numbers and  $n$  is the band index.  $S_{i\alpha, j\beta}$  is the overlap matrix and  $C_{j\beta}^n$  is the eigenvector of the wave function from the minimal basis calculations. The BO values depend mostly on the interatomic separations but can also be affected by the presence of other nearby atoms (bond angles). The strength of the IGF depends on the strength of the bonds and the number of bonds present. The change in the bond order density (BOD) in the IGF model as a function of strain is shown in Fig. 4(b). We define the BOD as the totality of the BOs of all bonds crossing a plane of small thickness perpendicular to the  $z$  axis. As can be seen, in the crystalline region, the distribution of BOD shows peaks and valleys as it passes through successive crystalline planes in  $\beta$ - $\text{Si}_3\text{N}_4$ . In the IGF region, the BOD is much lower than the averages in the crystalline region, reflecting the weaker Si–O bonds in the IGF compared to the highly covalent Si–N bonds in the crystal. As the strain is increased, the BOD decreases due to the longer and therefore weaker bonds and eventually the breaking of some of these bonds. The sizable stress remaining in the IGF model after it reaches the maximum can be accounted for by the remaining stress in the surfacial films due to the inherent disorder associated with the glassy nature of the film, evidenced by the remaining peaks and valleys in the BOD diagram near crystal surfaces.

The above results based on theoretical tensile experiments show complicated deformation and failure mechanisms in an IGF model in  $\beta$ - $\text{Si}_3\text{N}_4$  with prismatic surfaces.

The model is sufficiently large with a few defective structures. This is in contrast to an earlier study on the basal model which shows very different fracture behavior and failure mechanism.<sup>4–6</sup> This can be attributed to the fact that the basal IGF model has more defective atoms near the interface. It also shows that the bonding of atoms in the vicinity of the crystalline and IGF interfaces depends critically on the crystal orientations. Such differences which originate from the atomic scale structure and bonding of the IGF microstructures in ceramics have not been investigated so far. In the present work, the deformation behavior is accompanied by parallel calculation of the electronic structure and BODs. Such analysis is more accurate than those based purely on geometric configurations from classical simulations. Our results do reveal some surprises such as the similarities in the DOS for models under different strains and the formation of surfacial films after fracture. These facts are consistent with the belief that the formation of surfacial films and their accompanying thermodynamics is similar to the IGF formations in bulk polycrystalline materials.<sup>1</sup> Further results with more detailed descriptions will be reported in future publications.

This work is supported by the U.S. Department of Energy under Grant No. DE-FG02-84DR45170. This research used the resources of NERSC supported by the Office of Science of DOE under Contract No. DE-AC03-76SF00098.

<sup>1</sup>J. Luo, *Crit. Rev. Solid State Mater. Sci.* **32**, 67 (2007).

<sup>2</sup>S. Ogata, Y. Umeno, and M. Kohyama, *Modell. Simul. Mater. Sci. Eng.* **17**, 013001 (2009).

<sup>3</sup>P. Rulis, J. Chen, L. Ouyang, W. Y. Ching, X. Su, and S. H. Garofalini, *Phys. Rev. B* **71**, 235317 (2005).

<sup>4</sup>J. Chen, P. Rulis, L. Ouyang, A. Misra, and W. Y. Ching, *Phys. Rev. Lett.* **95**, 256103 (2005).

<sup>5</sup>W. Y. Ching, J. Chen, P. Rulis, L. Ouyang, and A. Misra, *J. Mater. Sci.* **41**, 5061 (2006).

<sup>6</sup>A. Misra, L. Ouyang, J. Chen, and W. Y. Ching, *Philos. Mag. A* **87**, 3839 (2007).

<sup>7</sup>P. F. Becher, G. S. Painter, E. Y. Sun, C. H. Hsueh, and M. J. Lance, *Acta Mater.* **48**, 4493 (2000).

<sup>8</sup>I. Tanaka, H.-J. Kleebe, M. K. Cinibulk, J. Bruley, D. R. Clarke, and M. Ruhle, *J. Am. Ceram. Soc.* **77**, 911 (1994).

<sup>9</sup>G. Kresse and J. Hafner, *Phys. Rev. B* **47**, 558 (1993); G. Kresse and J. Furthmuller, *Comput. Mater. Sci.* **6**, 15 (1996).

<sup>10</sup>N. Shibata, S. J. Pennycook, T. R. Gosnell, G. S. Painter, W. A. Shelton, and P. F. Becher, *Nature (London)* **428**, 730 (2004).

<sup>11</sup>A. Ziegler, J. C. Idrobo, M. K. Cinibulk, C. Kisielowski, N. D. Browning, and R. O. Ritchie, *Science* **306**, 1768 (2004).

<sup>12</sup>W. Walkosz, R. F. Klie, S. Ogut, A. Borisevich, P. F. Becher, S. J. Pennycook, and J. C. Idrobo, *Appl. Phys. Lett.* **93**, 053104 (2008).

<sup>13</sup>S. Ogata, N. Horosaki, C. Kocer, and H. Kitagawa, *Phys. Rev. B* **64**, 172102 (2001).

<sup>14</sup>W. Y. Ching, *J. Am. Ceram. Soc.* **73**, 3135 (1990).

<sup>15</sup>The full basis used for the present calculation consists of atomic orbitals  $1s$ ,  $2s$ ,  $3s$ ,  $4s$ ,  $2p$ ,  $3p$ ,  $4p$ , and  $3d$  for Si and  $1s$ ,  $2s$ ,  $3s$ ,  $2p$ , and  $3p$  for O and N. The core orbitals (Si  $1s$ ,  $2s$ ,  $2p$  and O–N  $1s$ ) are later orthogonalized to the noncore orbitals.

<sup>16</sup>R. S. Mulliken, *J. Chem. Phys.* **23**, 1841 (1955).